FOREX Publication
Open Access | Rapid and quality publishing

International Journal of
Electrical and Electronics Research (IJEER)
Research Article | Volume 11, Issue 1 | Pages 213-221 | e-ISSN: 2347-470X

Boundary-Based Hybrid Control Algorithm for Switched Boost Converter Operating in CCM and DCM

Hardik Patel[1] and Ankit Shah[2*]

[1]PhD Research Scholar, Gujarat Technological University, Ahmedabad and Assistant Professor, Instrumentation and Control Engineering Department, Government Engineering College, Rajkot, Gujarat, India, er.hardik24@gmail.com

[2]Instrumentation and Control Engineering Department, L. D. College of Engineering, Gujarat Technological University, Ahmedabad, Gujarat, India, ankitshah.ic@ldce.ac.in

***Correspondence:** Ankit Shah; ankitshah.ic@ldce.ac.in

ABSTRACT- It is essential to have enhanced efficiency for the DC-DC converters operating in continuous conduction mode (CCM) and discontinuous conduction mode (DCM). This requires a hybrid controller designed using pulse width modulation (PWM) and pulse frequency modulation (PFM) schemes. This paper fixates on a boundary-based hybrid control algorithm for the second-order DC-DC converter - the switched boost converter. The proposed algorithm works in PWM control scheme for CCM operation, whereas DCM operation uses PFM control scheme. The boundary conditions are defined by the load current, output voltage, and switching frequency. Here, an attempt is carried out to have the advantages of both the control schemes. The boost converter is represented by the switched system operating in three modes. Violating transition guards condition orchestrates the switching among these modes. A supervisor detects the CCM and DCM operations, and subsequently switches between PWM and PFM control scheme. Extensive circuit-level simulations are carried out in MATLAB to show the efficacy of the suggested algorithm under the fluctuating line, load, and set-point.

Keywords: Boost converter, continuous conduction mode, discontinuous conduction mode, hybrid control, switched system.

ARTICLE INFORMATION

Author(s): Hardik Patel and Ankit Shah;
Received: 31/01/2023; **Accepted**: 29/03/2023; **Published**: 30/03/2023;
e-ISSN: 2347-470X;
Paper Id: IJEER 3101-10;
Citation: 10.37391/IJEER.110129
Webpage-link:
www.ijeer.forexjournal.co.in/archive/volume-11/ijeer-110129.html

Publisher's Note: FOREX Publication stays neutral with regard to Jurisdictional claims in Published maps and institutional affiliations.

1. INTRODUCTION

The DC-DC converters gained an enormous interest in the last few decades as it widely used in numerous applications, *e.g.*, electric vehicles, computer laptops, cellular phones, photovoltaic systems, to name a few. Hence, the performance of DC-DC converter plays a significant role in the efficiency of these systems. Researchers do depth analysis of DC-DC converters in recent years. Usually, a transfer function is obtained by state-space analysis using small-signal models [1] [2] [3] [4], large signal models [5], and circuit averaging techniques [6] for control design. These models are derived at a nominal load; consequently, the efficiency is sacrificed because of changes in line and load conditions. The modeling for CCM and DCM is different, and most of the cases, DCM is overlooked [2] [3] [4] [5]. In some exceptional cases, merely critical condition mode (CrCM) is studied [7].

The converters normally operate in CCM under medium to high load and enter the DCM during light load conditions. In fixed frequency PWM controllers, driver and switching losses increase during light load conditions, and result in poorer efficiency [8]. To counteract this, frequency is lowered by PFM [9], constant on-time based PFM with fixed switching frequency for CCM [10], pulse skip modulation (PSM) [11], pulse train (PT) [12], multilevel pulse train (MPT) [13], and digital pulse width modulation (DPWM) [8]. Periodic event-triggered dynamic output feedback control with output quantization is suggested to reduce actuator wear and communication bandwidth in [14]. Because of advent in control theory, modern techniques like artificial intelligence based fuzzy control [15], min-type control [16], H-infinity technique [17], optimal control [18], sliding mode control (SMC) [19], and robust control [20] is also used for control design. However, most of these approaches use extensive mathematical computations and requires high-end processors for implementation.

Among different converters, boost and buck-boost converters have right half plane (RHP) zero, unlike buck converter. This system is called a non-minimum phase (NMP) system. The internal model control (IMC) scheme is implemented for such system and compared with the proportional integral derivative (PID) controller in [21]. The elimination of RHP zero is shown in [22]. As the switched boost converter exhibit NMP, inverse response is apparent, which makes controlling of boost converter even more complicated.

As an attempt to rectify the above issues, hybrid control algorithms were also introduced. An energy balance-based hybrid control [23] and PFM + Sinusoidal PWM based hybrid control [24] are suggested, but both are only applicable for DCM operation. A PFM based hybrid control algorithm is carried out in [25]. However, the PFM scheme is uniformly used for CCM and DCM operations. The result is too high switching

FOREX Publication
Open Access | Rapid and quality publishing
International Journal of Electrical and Electronics Research (IJEER)
Research Article | Volume 11, Issue 1 | Pages 213-221 | e-ISSN: 2347-470X

frequency in CCM operation, which rises driver and switching losses. The boost converter models in CCM and DCM are different in the frequency domain. Therefore, it is difficult to design a controller with stable operation for both modes. Thus, there is a need of control algorithm, which can work effectively in CCM and DCM operations with high efficiency. Being a fixed frequency scheme, the PWM scheme has more advantages as long as CCM operation is concerned, but it introduces high switching and driver losses when the converter operates in DCM [8]. To redress this, frequency is decreased by many ways as discussed earlier.

Here, the proposed algorithm employs PWM and PFM control schemes for CCM and DCM operations, respectively. As the control scheme switches to PFM at light load, switching and driver losses are decreased because of the lower switching frequency. The switched boost converter is shown as an interaction between continuous and discrete transitions and represented by hybrid automaton. The boundary conditions, which control the switching between different states and events of hybrid automaton, are defined by inductor current, switching frequency, and output voltage. The value of these parameters is called transition guards, which rests on line and load conditions. To control output voltage within limit, it involves a pertinent selection of transition guards.

2. MEDELLING OF SWITCHED BOOST CONVERTER

A typical boost converter is shown in *figure 1*. For analysis, following notations are used: *L*- inductor, *C*- capacitor, *R*– load resistance, MOSFET - Switch-1, Diode - Switch-2, *D*- gate pulses, *f*- switching frequency of switch-1, i_L- instantaneous inductor current, I_L- average value of i_L, Δi_L- ripple in i_L, I_{pk1}- peak value of i_L for CCM operation, I_{pk2}- peak value of i_L for DCM operation, V_{in}– average input voltage, i_C- instantaneous capacitor current, V_o- average output voltage, and v_o- instantaneous output voltage. By neglecting effective series resistance (ESR) of capacitor, $V_c = V_o$.

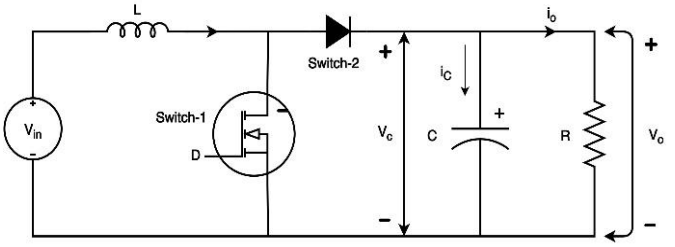

Figure 1: Typical switched boost converter circuit

The state-space equation is developed using the following definitions for a CCM-DCM operated switched boost converter. The input voltage is considered as a constant voltage unlike considered as a control input in most of works [4, 14, 23].

Let $X \in R^n$ be continuous state and k takes values in finite set $K \triangleq \{1,\ldots,N\}$ and is discrete state. $k \in K$ represents the on/off configuration of MOSFET and diode. For each $k \in K$, continuous dynamics is modeled by the differential equation as below:

$$\dot{x}(t) = A_k x(t) + B_k \tag{1}$$

Where $x \in X$ is state vector, $A_k \in R^{n\times n}$ is system matrix and $B_k \in R^{n\times 1}$.

The switched system is a special class of hybrid system [26] and mathematically switched dynamical systems can be described by [27],

$$\dot{x}(t) = f_\sigma\left(x(t)\right) \tag{2}$$

Where σ is taking values from index set $M \triangleq \{1,\ldots,m\}$ and m represents the number subsystems.

A hybrid automaton [28] can be defined by tuple *H={K, X, F, I, E, g, TG}* which has following components,

- $K=\{k_1,k_2,k_3\}$ is finite set of topologies.
- A state is defined by $F:(K\times X) \rightarrow R^n$.
- $I:K \rightarrow 2^X$ is a mapping that assigns an invariant set $I_k \subseteq X$ for each topology $k \in K$.
- $E \subseteq (K\times K)$ is a set of feasible discrete transitions (or events) allowed among the topologies, such that an element $e_{ij} = (k_i,k_j) \in E$ implies that a discrete transition from i^{th} topology to j^{th} topology is allowed.
- $g:E \rightarrow TG$ is guard function such that $e_{ij} \in E$ to corresponding to guard $g(e_{ij}) \in TG$.
- $TG:E \rightarrow 2^X$ is transition guard such that for each $e_{ij} \in E$; $\exists$ $g(e_{ij}) \in TG$.

Table 1: Possible discrete state in switched boost Converter

Discrete state	Switch-1	Switch-2
k_1	ON	OFF
k_2	OFF	ON
k_3	OFF	OFF
k_4	ON	ON

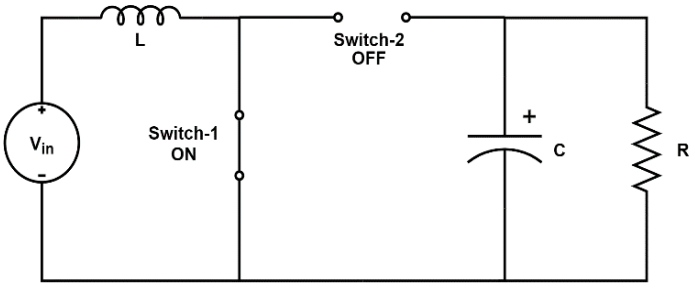

(a)

FOREX Publication
Open Access | Rapid and quality publishing
International Journal of Electrical and Electronics Research (IJEER)
Research Article | Volume 11, Issue 1 | Pages 213-221 | e-ISSN: 2347-470X

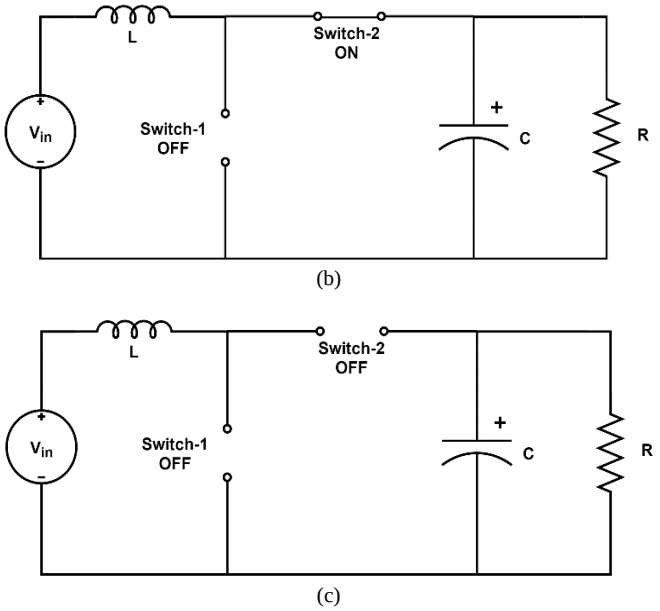

Figure 2: Switched boost converter circuit in different discrete states (a) Mode-k_1 (b) Mode- k_2 (c) Mode- k_3

As there are two switches present in the circuit, 2^n discrete states are possible. Thus, the second order switched boost converter has four discrete states as mentioned in *table-1*, and the corresponding circuit for each state is shown in *figure 2*.

Among these states, k_4 is not practicable. Then, $K = \{k_1, k_2, k_3\}$ are possible discrete state, whereas E = $[(k_1, k_2), (k_2, k_1), (k_2, k_3), (k_3, k_1)]$ are likely events. Out of these, $\{(k_1, k_2), (k_2, k_1)\}$ corresponds to CCM operation and $\{(k_1, k_2), (k_2, k_3), (k_3, k_1)\}$ corresponds to DCM operation of the switched boost converter.

Table 2: System state matrices corresponding to operating modes

Operating Mode (k_i)	A_i	B_i
k_1	$\begin{bmatrix} 0 & 0 \\ 0 & -\frac{1}{RC} \end{bmatrix}$	$\begin{bmatrix} \frac{V_{in}}{L} \\ 0 \end{bmatrix}$
k_2	$\begin{bmatrix} 0 & -\frac{1}{L} \\ \frac{1}{C} & -\frac{1}{RC} \end{bmatrix}$	$\begin{bmatrix} \frac{V_{in}}{L} \\ 0 \end{bmatrix}$
k_3	$\begin{bmatrix} 0 & 0 \\ 0 & -\frac{1}{RC} \end{bmatrix}$	$\begin{bmatrix} 0 \\ 0 \end{bmatrix}$

In *figure 1*, i_L and v_o are the system state variables. It brings three state equations corresponding to $K_i = (i = 1, 2, 3)$ as shown in *table 2*.

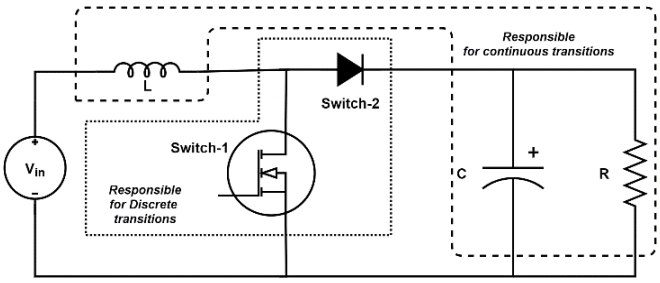

Figure 3: The behavior of components in switched boost converter

The switched boost converter exhibits both continuous and discrete behavior because the circuit comprises passive components and switches, as shown in *figure 3*. So, a hybrid automaton can represent it as shown in *figure 4*. H_1 and H_2 represents discrete and continuous transitions, respectively. While H_1 depends on the continuous signal x from H_2, H_2 accepts the discrete value $\sigma \in \Sigma$ from H_1 and the continuous state x grows accordingly.

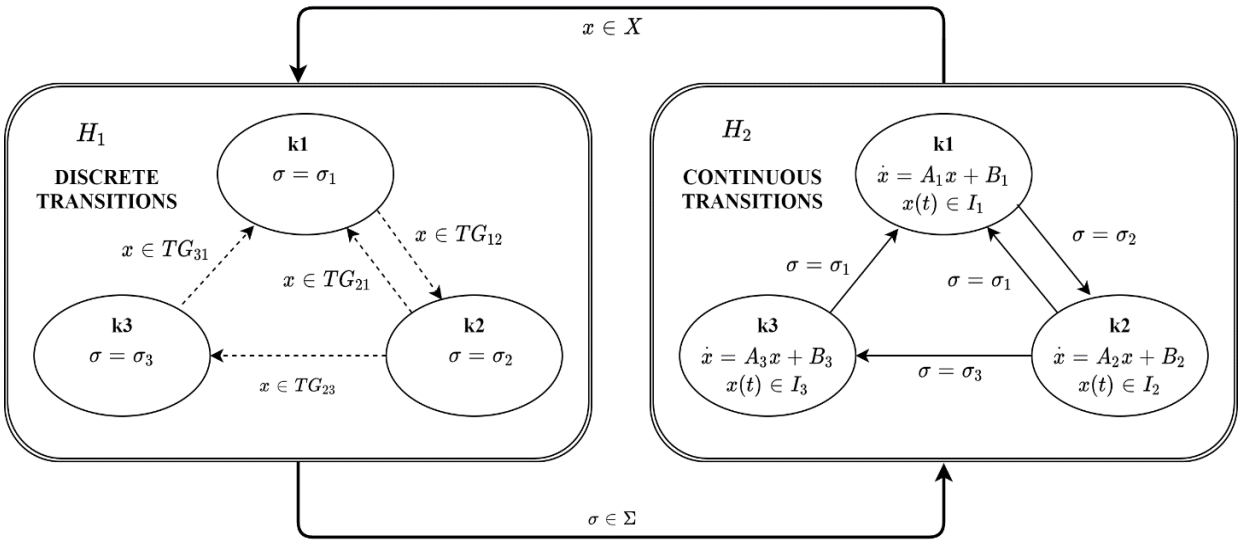

Figure 4: Hybrid automaton representation of switched boost converter shown as an interaction of continuous and discrete transitions

FOREX Publication
Open Access | Rapid and quality publishing
International Journal of Electrical and Electronics Research (IJEER)
Research Article | Volume 11, Issue 1 | Pages 213-221 | e-ISSN: 2347-470X

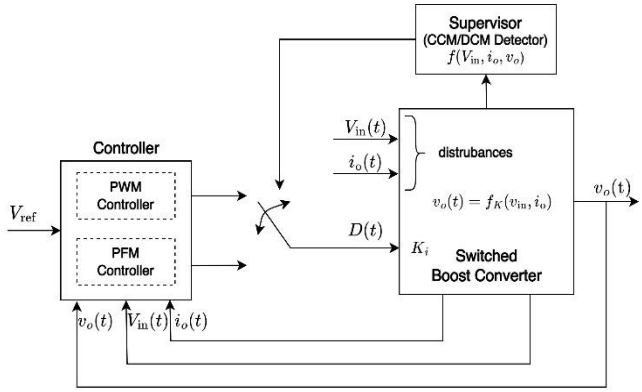

Figure 5: Hybrid control scheme for switched boost converter in the closed-loop

3. BOUNDARY BASED HYBRID CONTROLLER DESIGN

A boundary-based control scheme is presented with simple and nominal mathematical computations. As there are three modes present, three transition guards named TG_{12}, TG_{23} and TG_{31} considered here to control switching between three modes as shown in *figure 4*. The selection of proper transition guards makes sure that the state trajectories kept within the limit. The only difference between CCM and DCM operations is, TG_{31} is not declared in CCM. The proposed controller architecture is hybrid by using PWM and PFM control schemes for CCM and DCM operations, respectively. *Figure 5* shows the resulting closed-loop hybrid control scheme.

3.1 PWM Controller Design for CCM Operation

Approximated waveforms of inductor current and output voltage of the switched boost converter operating in CCM is shown in *figure 6*.

Here, transition guards need to be selected such that fixed frequency PWM control scheme is implemented.

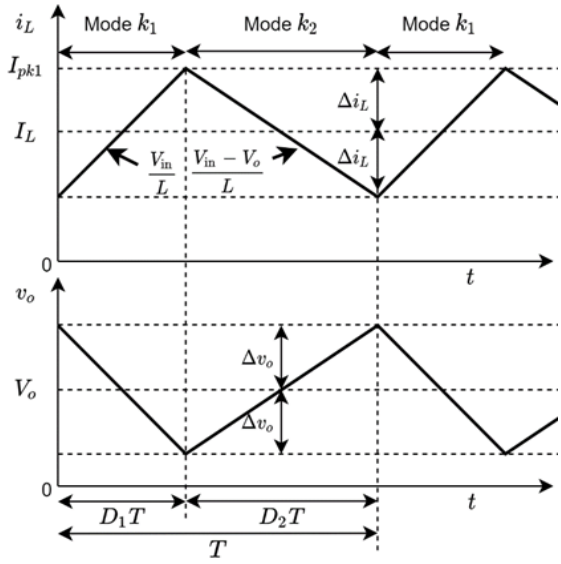

Figure 6: Approximated waveforms of state variables in CCM

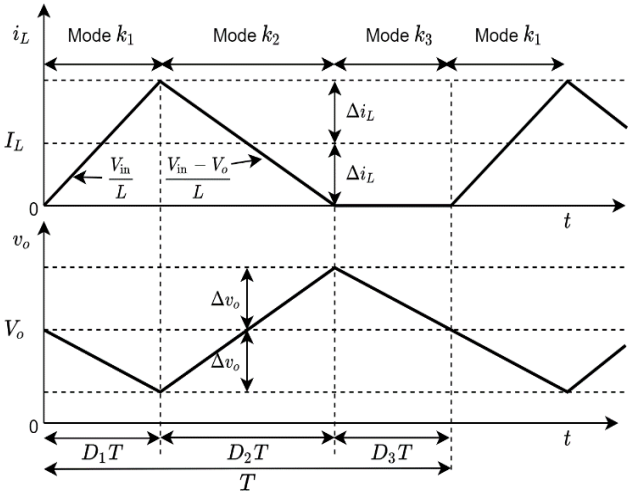

Figure 7: Approximated waveforms of state variables in DCM

At steady state, the average output voltage for boost converter can be written as,

$$V_o = \frac{V_{in}}{1-D} \tag{3}$$

During mode-k_1, input voltage V_{in} appears across the inductor, which causes a change in inductor current. The change in i_L during this time ($\Delta t = D_1T$) is written as;

$$\frac{2\Delta i_L}{\Delta t} = \frac{V_{in}}{L} \tag{4}$$

By using (3) and (4), the ripple current is calculated as below:

$$\Delta i_L = \frac{V_{in}(V_o - V_{in})}{2LfV_o} \tag{5}$$

The average inductor current - I_L can be derived by equating input and output power as below:

$$V_{in} \times I_L = V_0 \times I_o \tag{6}$$

The I_L is derived from (6) as follows:

$$I_L = \frac{V_o^2}{RV_{in}} \tag{7}$$

From *figure 6*, peak inductor current during CCM operation can be given as;

$$I_{pk1} = I_L + \Delta i_L \tag{8}$$

From *eq. (8)*, peak current of the inductor depends on line and load conditions and it is considered as TG_{12}: $i_L \geq I_{pk1}$ to control transition from mode-k_1 to mode-k_2. The transition from mode-k_2 to mode-k_1 is determined by TG_{21}: $t \geq T$, where T is the time period.

FOREX Publication
Open Access | Rapid and quality publishing
International Journal of Electrical and Electronics Research (IJEER)
Research Article | Volume 11, Issue 1 | Pages 213-221 | e-ISSN: 2347-470X

3.2 Supervisor (CCM/DCM Detector)

Here, the supervisor must be designed to distinguish the CCM and DCM operations. While the inductor current is invariably greater than zero in CCM operation, it becomes zero for a short period of time in DCM operation. The latter condition occurs when the ripple current of inductor is higher than average inductor current. Thus, different operating modes are summarized as; $I_L > \Delta i_L \Rightarrow$ CCM operation, $I_L < \Delta i_L \Rightarrow$ DCM operation and $I_L = \Delta i_L \Rightarrow$ CrCM operation.

3.3 PFM Controller Design for DCM Operation

At light load condition, the inductor drains its total energy before the completion of switching cycle is called DCM operation. *Figure 7* shows approximated inductor current and output voltage waveforms for DCM operation.

From volt-sec balance, the D_2 is calculated as follows:

$$D_2 = \frac{D_1 V_o}{V_o - V_{in}} \tag{9}$$

During D_2 T time, the average load current is the current passing through the diode and it can be expressed as;

$$\frac{V_{in} D_1 D_2}{2Lf} = \frac{V_o}{R} \tag{10}$$

We get the quadratic equation by using *eq. (9) and (10)* as below:

$$V_o^2 - V_o V_{in} - \frac{V_{in}^2 D_1^2 R}{2Lf} = 0 \tag{11}$$

By rearranging the feasible solution of quadratic *equation (11)*, D_1 is written as follows:

$$D_1 = \frac{1}{V_{in}} \sqrt{\frac{2V_o(V_o - V_{in})Lf}{R}} \tag{12}$$

From *eq. (12)* and *figure 7*, the peak current of inductor for DCM operation is calculated as follows:

$$I_{pk2} = \sqrt{\frac{2V_o(V_o - V_{in})}{RLf}} \tag{13}$$

Thus, the peak current as per *eq. (13)* determine the transition from mode-$k1$ to mode-$k2$. The transition from mode-k_2 to mode-k_3 is natural, and output voltage swing is considered for transition from mode-k_3 to mode-k_1. Thus, the transition guards for DCM operation are $TG_{12:}$ $i_L \geq I_{pk2}$, $TG_{23:}$ $i_L = 0$ and $TG_{31:}$ $v_o = V_o$.

$$f = \frac{V_o - V_{in}}{2\Delta v_o RC} \tag{14}$$

4. SIMULATION RESULTS AND DISCUSSION

The simulation of proposed hybrid control scheme is implemented in MATLAB. The nominal parameters are V_{in} = 15 V, L =100 µH, C = 80 µF, R = 20 Ω, and V_o = 30 V. *Figure 8* shows the flow chart for the proposed scheme. The potency of the suggested control scheme is given by substantial amount of line and load variations as shown in *figure 9*. *Table 3* shows duty cycle (D), percentage of peak overshoot ($\%M_p$), and settling time (T_s) during different line, load and set-point changes. Detailed results are discussed in following subsections.

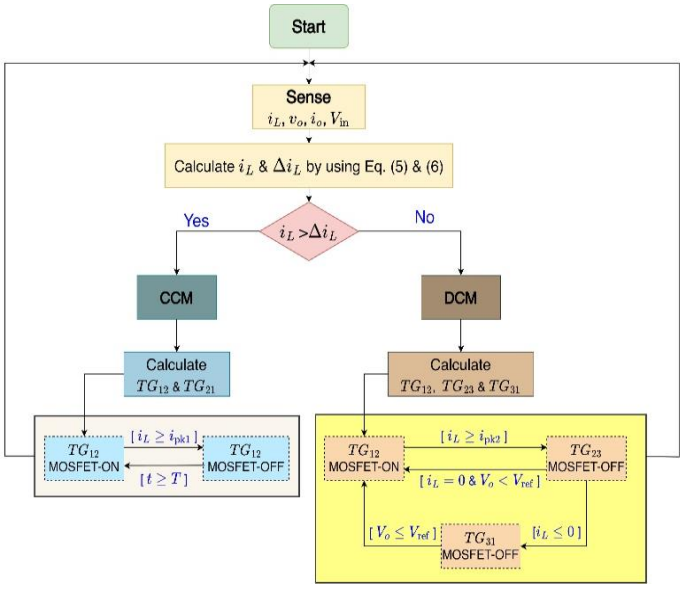

Figure 8: Flow chart of boundary-based hybrid control algorithm for switched boost converter

Table 3: D, M_p, and T_s during line, load and set-point variations

S. No.	Time span *(ms)*	R *(Ω)*	V_{in} *(V)*	V_{ref} *(V)*	D *(%)*	M_p *(%)*	T_s *(ms)*
1	[0-3)	20	15	30	[0-46.4)	0	2.5
2	[3-4)	20	17	30	[46.4-44.5)	0	0
3	[4-6)	30	17	30	[44.5-43.8)	0.6	0.1
4	[6-10)	30	17	32	[43.8-46.9)	0	3.5
5	[10-12)	37.7	17	32	[46.9-47.1)	0.4	0
6	[12-13)	100	17	32	[47.1-28.8)	1	0
7	[13-15)	100	17	30	[28.8-16.8)	0	0.6
8	[15-17)	500	15	30	[16.8-9.7)	0	0
9	[17-21)	1000	15	30	[9.7-6.5)	0	0
10	[21-25)	37.7	15	30	[6.5-4.9)	0.6	1

FOREX Publication
Open Access | Rapid and quality publishing
International Journal of Electrical and Electronics Research (IJEER)
Research Article | Volume 11, Issue 1 | Pages 213-221 | e-ISSN: 2347-470X

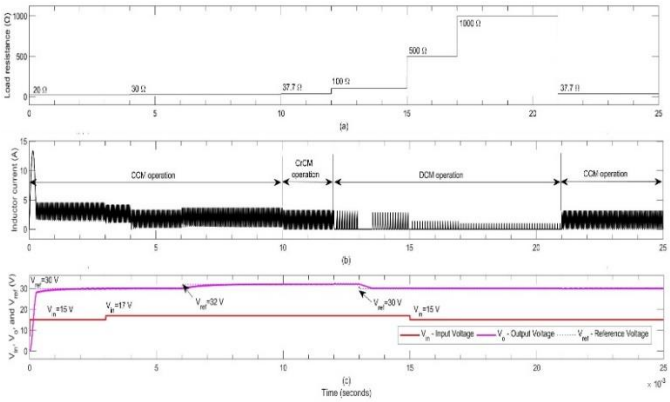

Figure 9: Simulation results: variations in (a) load resistance, (b) inductor current, (c) input voltage (red), reference voltage (blue) and output voltage (pink)

4.1 CCM Operation

Simulation is initiated at t = 0 with V_{in} = 15 V, R = 20 Ω, V_{ref} = 30 V, and 25 kHz switching frequency. At the turned-on instant, the output voltage of the switched boost converter quickly tracks set-point with no overshoot. The overall disturbances and results during the CCM operation are summarized below.

- The line voltage variation is given at t = 3ms from V_{in} = 15 V to 17 V. *Figure 10(a)* shows corresponding i_L and v_o, and no overshoot is observed in output voltage waveform.
- The load variation from R = 20 Ω to 30 Ω is given at t = 4 ms, and *figure 10(b)* shows the corresponding i_L and v_o waveforms. The output voltage fast settles to the desired value with negligible overshoot.
- To test the voltage tracking capability of the controller in CCM operation, set-point change from V_{ref} = 30 V to 32 V is given at t = 6ms. Corresponding variations of state variables are shown in *figure 10(c)*. The output voltage settles to a new set-point within 4ms.

Abruptly load is decreased to R = 37.7 Ω from 1000 Ω at t = 21ms to check the effectiveness of control scheme when switching from DCM to CCM operation. Even in this worst-incident, output voltage is restrained, as shown in *figure 10(d)*.

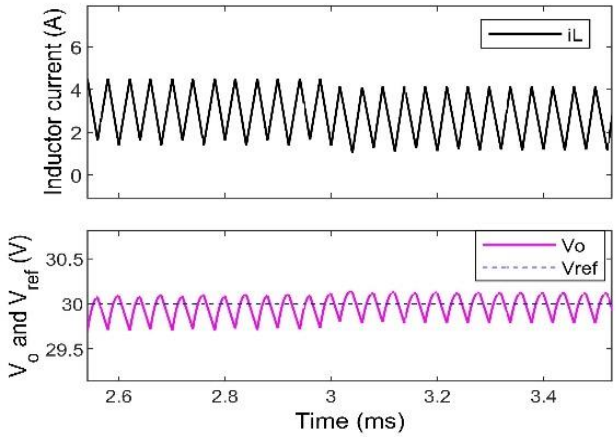

(a)

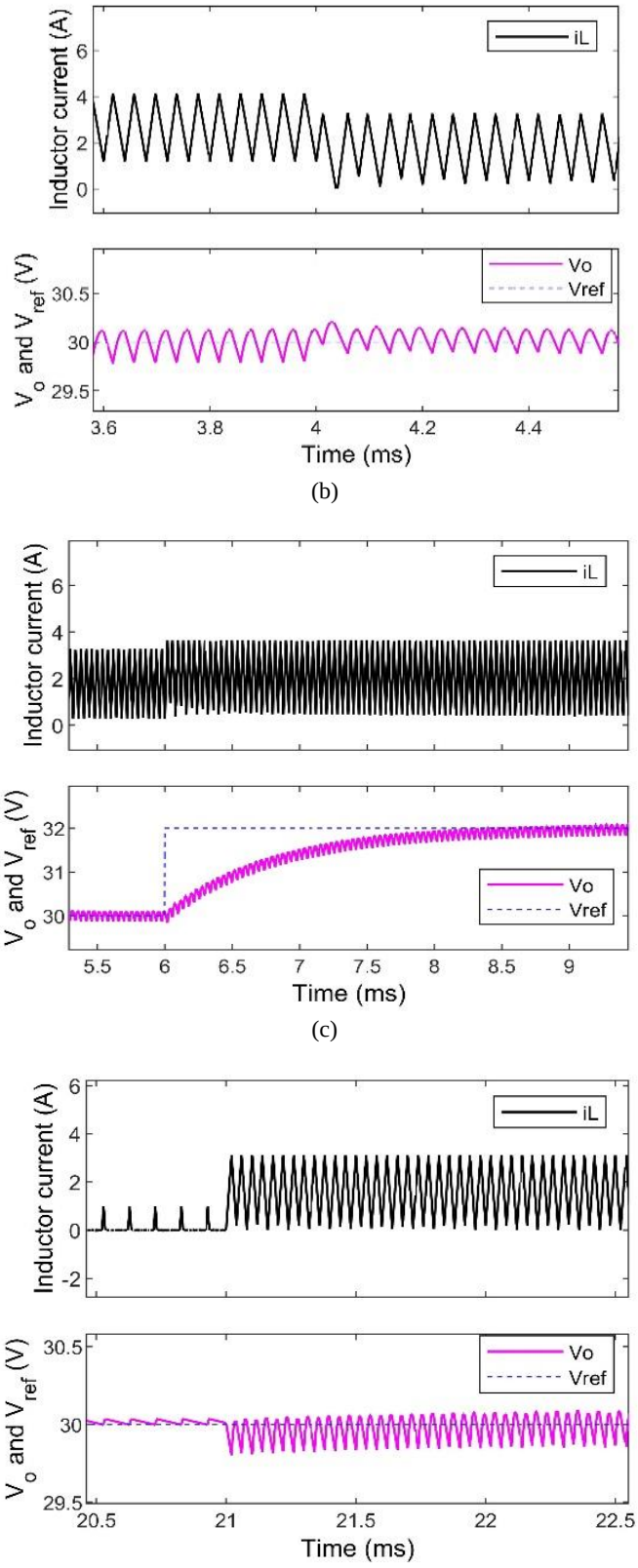

(b)

(c)

(d)

Figure 10: State variables transients during disturbances in CCM (a) For step-up change in V_{in} from 15 V to 17 V at t=3ms (b) For step-up change in R from 20 Ω to 30 Ω at t=4ms (c) For step-up change in set-point (V_{ref}) from 30 V to 32 V at t=6ms (d) For step-down change in R from 1000 Ω to 37.7 Ω at t=21ms.

FOREX Publication
Open Access | Rapid and quality publishing
International Journal of Electrical and Electronics Research (IJEER)
Research Article | Volume 11, Issue 1 | Pages 213-221 | e-ISSN: 2347-470X

4.2 CrCM Operation

Because of line and load fluctuations, if inductor current just becomes zero, and instantly rises again is called CrCM operation, also cited as boundary conduction mode (BCM) [7]. *Figure 11* shows state variables waveforms for step change in load from R = 30 Ω to 37.7 Ω at t = 10ms. Output voltage variation is not apparent with approximately zero steady-state error, and it does not struggle to track reference voltage.

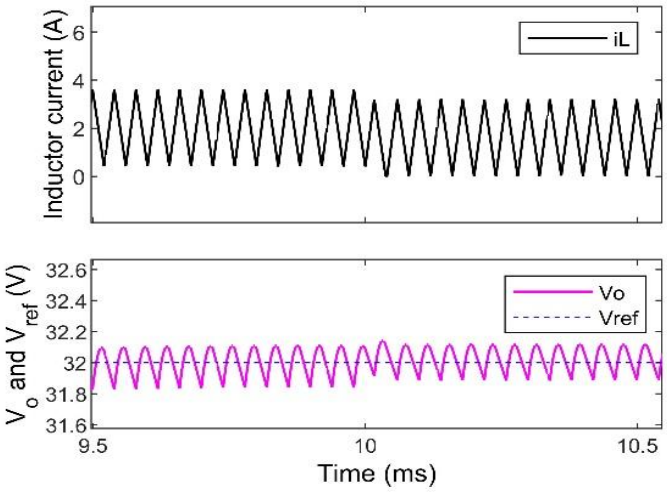

Figure 11: Variation of *iL* and *Vo* for step change in R from 30 Ω to 37.7 Ω at t = 10ms causing the CrCM operation

4.3 DCM Operation

A frequency of 10 kHz is selected to diminish losses during DCM operation. The disturbances during DCM operation are summarized below.

- At t = 12ms, abruptly load resistance is raised to R = 100 Ω from 37.7 Ω, which results in perfect DCM operation. The corresponding waveforms of i_L and v_o are shown in *figure 12(a)*.
- A negative set-point change from V_{ref} = 32 V to 30 V is given at t = 13ms to study the voltage tracking capability of the controller in DCM operation as well. *Figure 12(b)* shows, for nearly 1ms inductor current is not present, and the capacitor is providing energy to the load during this time. As output voltage is higher than reference voltage, switch-1 (MOSFET) is OFF, and the switch-2 (diode) blocks the back-flow of current.
- The reliability and robustness of the controller is further explored by the simultaneously changing line and load conditions. At t = 15ms, while load is increased from R = 100 Ω to 500 Ω, input voltage is decreased from V_{in} = 17 V to 15 V. Even in this condition, the output is under control, and no over or undershoot is evident as shown in *figure 12(c)*.

Load is further increased to R = 1000 Ω from 500 Ω at t = 17ms, and the controller effectively tracks the output voltage as shown in *figure 12(d)*.

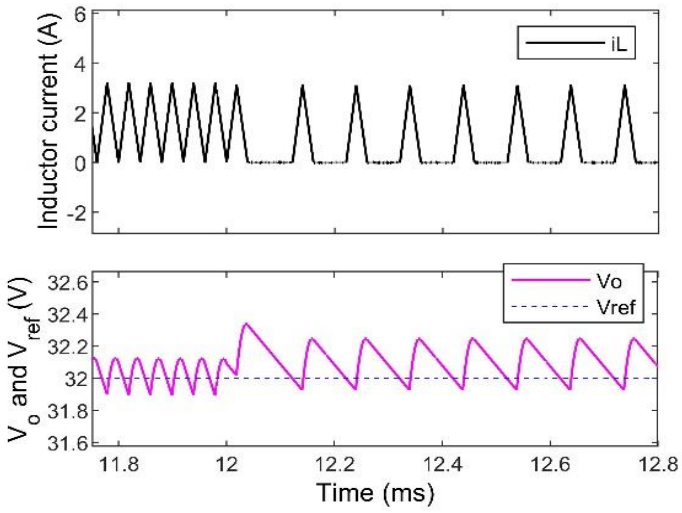

(a)

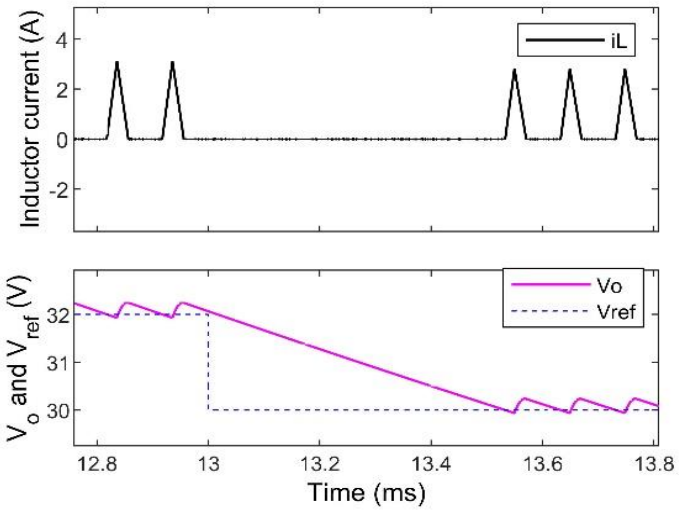

(b)

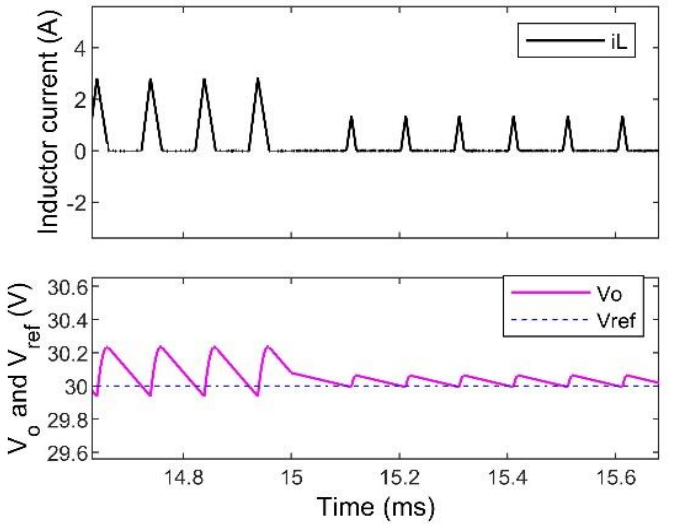

(c)

FOREX Publication
Open Access | Rapid and quality publishing
International Journal of Electrical and Electronics Research (IJEER)
Research Article | Volume 11, Issue 1 | Pages 213-221 | e-ISSN: 2347-470X

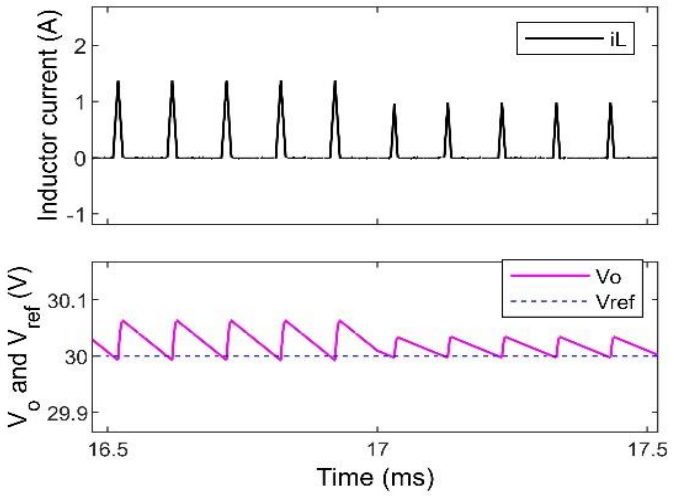

(d)

Figure 12: State variables transients during disturbances in DCM (a) For step change in R from 37.7 Ω to 100 Ω at t=12ms (b) For step-down change in set-point (V_{ref}) from 32 V to 30 V at t=13ms (c) For simultaneous step-up change in R from 100 Ω to 500 Ω and step-down change in V_{in} from 17 V to 15 V at t=15ms (d) For step-up change in R from 500 Ω to 1000 Ω at t=17ms

5. CONCLUSION

This paper presents a boundary-based hybrid control algorithm for the switched boost converter with simple and minimum mathematical calculations. The switched boost converter is represented by hybrid automaton working in three modes, and the transition guards are selected for switching among these modes. The circuit-level simulation of proposed control scheme is verified using MATLAB. Discrete transitions are implemented using state flow chart feature of MATLAB. Various positive and negative step changes in disturbances are given during CCM as well as in DCM operations. The transient and steady state output voltage responses are found satisfactory under disturbances and reference voltage variations. The proposed control scheme handles CrCM operation effectively, and output voltage variations are not found. Although, here only boost converter is considered, the scheme can be extended to other DC-DC converters, such as buck, buck-boost.

REFERENCES

[1] Corti, Fabio, et al. "Modelling of a pulse-skipping modulated DC–DC buck converter." IET Power Electronics, vol. 16, no. 2, pp. 243-254, 2023. https://doi.org/10.1049/pel2.12379

[2] A. Ayachit and M. K. Kazimierczuk, "Averaged small-signal model of pwm dc-dc converters in ccm including switching power loss", IEEE Transactions on Circuits and Systems II: Express Briefs, vol. 66, no. 2, pp. 262–266, 2019. https://doi.org/10.1109/TCSII.2018.2848623

[3] B. Bryant and M. K. Kazimierczuk, "Open-loop power-stage transfer functions relevant to current-mode control of boost PWM converter operating in CCM", IEEE Transactions on Circuits and Systems I: Regular Papers, vol. 52, no. 10, pp. 2158–2164, 2005. https://doi.org/10.1109/TCSI.2005.852919

[4] S. C. Smithson and S. S. Williamson, "A unified state-space model of constant-frequency current-mode-controlled power converters in continuous conduction mode", IEEE Transactions on Industrial Electronics, vol. 62, no. 7, pp. 4514–4524, 2015. https://doi.org/10.1109/TIE.2015.2412514

[5] H. Al-Baidhani, M. K. Kazimierczuk, and A. Reatti, "Nonlinear modeling and voltage-mode control of dc-dc boost converter for ccm", in Proceeding of IEEE International Symposium on Circuits and Systems (ISCAS), pp. 1–5, 2018. https://doi.org/10.1109/ISCAS.2018.8351078

[6] Y.-J. Mao, C.-S. Lam, S.-W. Sin, M.-C. Wong, and R. P. Martins, "Review and selection strategy for high-accuracy modeling of PWM converters in DCM", Journal of Electrical and Computer Engineering, vol. 2018, pp. 1-16, 2018. https://doi.org/10.1155/2018/3901693

[7] M. Biglarbegian, N. Kim, and B. Parkhideh, "Boundary conduction mode control of a boost converter with active switch current-mirroring sensing", IEEE Transactions on Power Electronics, vol. 33, no. 1, pp. 32–36, 2018. https://doi.org/10.1109/TPEL.2017.2716934

[8] B. C. Mandi, S. Kapat, and A. Patra, "Unified digital modulation techniques for dc–dc converters over a wide operating range: Implementation, modeling, and design guidelines", IEEE Transactions on Circuits and Systems I: Regular Papers, vol. 65, no. 4, pp. 1442–1453, 2018. https://doi.org/10.1109/TCSI.2017.2753539

[9] H. Chen, H. Huang, S. Jheng, H. Huang, and Y. Huang, "High-efficiency pfm boost converter with an accurate zero current detector", IEEE Transactions on Circuits and Systems II: Express Briefs, vol. 65, no. 11, pp. 1644–1648, 2018. https://doi.org/10.1109/TCSII.2017.2754514

[10] Xiaoru Xu, Xiaobo Wu, and Xiaolang Yan, "A quasi fixed frequency constant on time controlled boost converter", in Proceeding of IEEE International Symposium on Circuits and Systems, pp. 2206–2209, 2008. https://doi.org/10.1109/ISCAS.2008.4541890

[11] S. Nguyen, K. Yuk, and R. Amirtharajah, "Pulse skipping modulation method for multiple input buck boost converter", in Proceeding of IEEE 19th Wireless and Microwave Technology Conference (WAMICON), pp. 1–4, 2018. https://doi.org/10.1109/WAMICON.2018.8363919

[12] G. Zhou, W. Tan, S. Zhou, Y. Wang, and X. Ye, "Analysis of pulse train controlled pccm boost converter with low frequency oscillation suppression", IEEE Access, vol. 6, pp. 68 795–68 803, 2018. https://doi.org/10.1109/ACCESS.2018.2879888

[13] Ming Qin, Jianping Xu, and Fei Zhang, "Analysis of multilevel pulse train control technique for boost converter operating in discontinuous conduction mode", in Proceeding of IEEE 6th International Power Electronics and Motion Control Conference, pp. 1353–1356, 2009. https://doi.org/10.1109/IPEMC.2009.5157594

[14] G. Ma and P. R. Pagilla, "Periodic event-triggered dynamic output feedback control of switched systems", Nonlinear Analysis: Hybrid Systems, vol. 31, pp. 247 – 264, 2019. https://doi.org/10.1016/j.nahs.2018.10.001

[15] B Raja Sekhar Reddya, V.C Veera Reddyb, M. VijayaKumar, "Modelling and Analysis of DC-DC Converters with AI Based MPP Tracking Approaches for Grid-Tied PV-Fuel Cell System." Electric Power Systems Research, vol. 216, pp. 1-9, 2023. https://doi.org/10.1016/j.epsr.2022.109053

[16] A. Sferlazza, C. Albea-Sanchez, L. Mart´ınez-Salamero, G. Garc´ıa, and C. Alonso, "Min-type control strategy of a dc–dc synchronous boost converter", IEEE Transactions on Industrial Electronics, vol. 67, no. 4, pp. 3167–3179, 2020. https://doi.org/10.1109/TIE.2019.2908597

[17] Q. Su and J. Zhao, "H∞ control for a class of continuous-time switched systems with state constraints", Asian Journal of Control, vol. 16, no. 2, pp. 451–460, 2014. https://doi.org/10.1002/asjc.706

[18] Mitra, Lopamudra, and Ullash Kumar Rout. "Optimal control of a high gain DC-DC converter", International Journal of Power Electronics and Drive Systems, vol. 13, no. 1, pp. 256-266, 2022. http://doi.org/10.11591/ijpeds.v13.i1.pp256-266

[19] Y. Massaoudi, E. Dorsaf, J.-P. Gaubert, D. Mehdi, and T. Damak, "Experimental implementation of new sliding mode control law applied to a dc–dc boost converter", Asian journal of control, vol. 18, no. 6, pp. 2221–2233, 2016. https://doi.org/10.1002/asjc.1318

[20] P. Song, C. Cui, and Y. Bai, "Robust output voltage regulation for dc– dc buck converters under load variations via sampled-data sensor less control", IEEE Access, vol. 6, pp. 10688–10698, 2018. https://doi.org/10.1109/ACCESS.2018.2794458

International Journal of
Electrical and Electronics Research (IJEER)
Research Article | Volume 11, Issue 1 | Pages 213-221 | e-ISSN: 2347-470X

[21] T. Kobaku, S. C. Patwardhan, and V. Agarwal, "Experimental evaluation of internal model control scheme on a dc–dc boost converter exhibiting nonminimum phase behavior", IEEE Transactions on Power Electronics, vol. 32, no. 11, pp. 8880–8891, 2017. https://doi.org/10.1109/TPEL.2017.2648888

[22] A. Goudarzian, A. Khosravi, and H. A. Raeisi, "Modeling and implementation of a new boost converter with elimination of right-halfplan zero", International Transactions on Electrical Energy Systems, vol. 30, no. 9, pp. 1-33, 2020. https://doi.org/10.1002/2050-7038.12476

[23] P. Gupta and A. Patra, "Hybrid mode-switched control of dc-dc boost converter circuits", IEEE Transactions on Circuits and Systems II: Express Briefs, vol. 52, no. 11, pp. 734–738, 2005. https://doi.org/10.1109/TCSII.2005.852189

[24] L. Qin, B. Duan, J. L. Soon, W. Hassan, J. Shen and L. Zhang, "Hybrid PFM and SPWM Control Scheme for DCM Single-Leg-Integrated Boost Inverter", IEEE Transactions on Industrial Electronics, pp. 1-10, 2023. https://doi.org/10.1109/TIE.2023.3236094

[25] C. Sreekumar and V. Agarwal, "A hybrid control algorithm for voltage regulation in dc–dc boost converter", IEEE Transactions on Industrial Electronics, vol. 55, no. 6, pp. 2530–2538, 2008. https://doi.org/10.1109/TIE.2008.918640

[26] J. Lu, Z. She, W. Feng, and S. S. Ge, "Stabilizability of time-varying switched systems based on piecewise continuous scalar functions", IEEE Transactions on Automatic Control, vol. 64, no. 6, pp. 2637–2644, 2019. https://doi.org/10.1109/TAC.2018.2867933

[27] Z. Sun and S. S. Ge, Stability theory of switched dynamical systems. Springer Science & Business Media, 2011, ch. 1.

[28] A. J. Van Der Schaft and J. M. Schumacher, "An introduction to hybrid dynamical systems" Springer London, 2000, ch. 1.